# Investigation of Cable Insulation and Thermo-Mechanical Properties of $Nb_3Sn$ Composite

D.R. Chichili, T.T. Arkan, J.P. Ozelis and I. Terechkine

***Abstract*--Within the framework of the Fermilab high field magnet program, cable insulation and thermo-mechanical properties of epoxy impregnated $Nb_3Sn$ composite were studied. As a part of cable insulation development, a new wrappable ceramic insulation developed by Composite Technology Development Inc. (CTD) was investigated to understand its mechanical properties and influence on magnet fabrication technology. Additionally, thermo-mechanical properties of the $Nb_3Sn$ composite made out of ten-stack samples were studied. Measurements of modulus of elasticity and Poisson's ratio were made under compression at room temperature and at 4.2 K. The results from both monotonic and cyclic loading tests are presented. Finally, measurements of the coefficient of thermal contraction for the composite using strain gauges is discussed.**

## I. Introduction

Fermilab, in collaboration with LBNL and KEK, is developing a high field $Nb_3Sn$ dipole for use in the next generation Hadron Collider. The conceptual design for the first magnet, detailed elsewhere [1], is based on a 2-layer cosθ coil structure and cold iron yoke. As a part of this program, various issues such as cable insulation, epoxy impregnation and thermo-mechanical properties of the composite are being investigated.

Knowledge of the behavior of cable insulation and the thermo-mechanical mechanical properties of the composite is essential for the mechanical design of the magnet as they provide a means to estimate the prestress under warm conditions, losses due to differential thermal contraction during cool down and finally the stresses developed due to Lorentz forces during excitation.

## II. Cable Insulation

A new wrappable ceramic insulation developed by CTD was investigated as a possible candidate for cable insulation [2]. Unlike traditionally used S-2 fiber glass insulation, this insulation does not have any organic binder thus requiring no heat-treatment. However, winding tests showed insulation damage especially in the areas where the cable was wound around the end-parts. To avoid this damage, ceramic binder (CTD-1002x) [3] was applied to the insulation and cured at 80 $^{o}$C for 20 min [4]. But this resizing of insulation increased the thickness anywhere from 125 to 225 μm depending upon the method of application of the binder. Based on the repeatability tests and insulation thickness requirements, Method 3 (Fig. 1) was chosen. Winding tests also revealed that butt lap (0% overlap) have the tendency to create turn to turn shorts due to insulation spreading near the ends. However with insulation overlap this problem was solved. It was decided to go with 50% overlap for the first dipole model [1] which gives an average insulation thickness of about 250 μm (Fig. 2) at impregnation pressure.

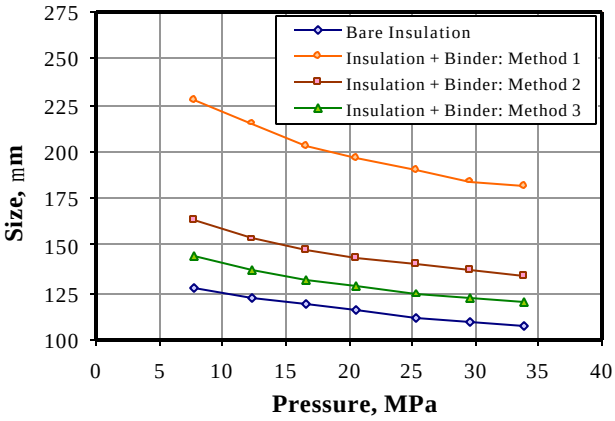


**Figure 1**: *Variation of the insulation thickness with binder application. Method 1: Insulation was dipped in the binder and then wrapped around the cable; Method 2: Cable was wrapped with insulation and then binder was applied with a brush; Method 3: Cable was wrapped with insulation and then binder was applied using a roller.*

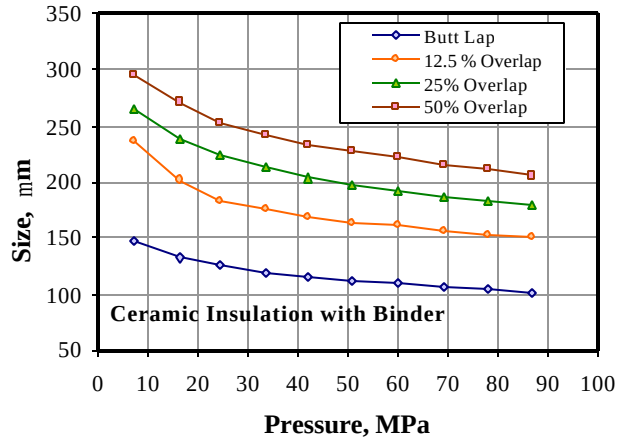


**Figure 2:** *Variation of mean insulation thickness with percentage overlap.*

Technical Division, Fermilab, Batavia, IL 60510 (USA).
Work is supported by the U.S. Department of Energy

## III. Mechanical Properties

Insulated ten-stack samples were reacted and then vacuum impregnated with CTD-101K [3]. Fig. 3 shows an epoxy impregnated composite with direction convention used in this paper. Strain gauges were mounted to measure strains both in the direction of load and transverse to the direction of the load. A calibrated load cell was used to record the force applied on the sample. To validate the testing fixture and strain gauge mounting technique, elasticity modulus of 6061-T651 aluminum and ULTEM 2300 were measured and compared with published literature [5]. Table 1 lists these values. Note that the measured values compare well with the published data.

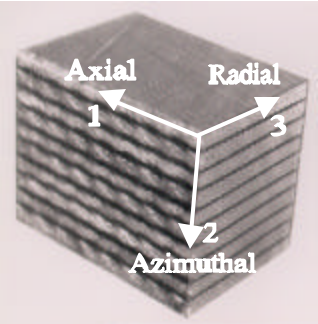


**Figure 3**: *Epoxy impregnated ten-stack composite.*

| MATERIAL | MEASURED | PUBLISHED |
|---|---|---|
| 6061-T651 Al | 68.5 GPa | 70.0 GPa |
| ULTEM 2300 | 6.7 GPa | 6.5 GPa |

**Table 1**: *Modulus measurements for 6061-T651 Aluminum and ULTEM 2300.*

Mechanical properties of the $Nb_3Sn$ composite were measured along all the three directions; azimuthal, axial and radial. Identical tests were done on more than one sample to check the repeatability. The stress-strain curves were repeatable within 2-4%. Both monotonic and cyclic loading tests were performed at 300 K and at 4.2 K and the test results are discussed below.

### *A. Azimuthal Direction: Monotonic Loading*

The behavior of the overall composite in azimuthal direction depends on all the individual constituents unlike in axial and radial direction where the behavior is mainly dominated by the $Nb_3Sn$ conductor. Fig. 4 shows the test results at room temperature for the composite with ceramic and with S-2 fiber glass insulation. Note that the stiffness with ceramic insulation is slightly higher than with S-2 fiber glass. However, in both cases, the composite exhibits non-linear behavior. Further the impregnation pressure in the range of 10 to 50 MPa had no effect on the mechanical behavior of the composite. Also shown in the figure is the behavior of the $Nb_3Sn$ composite which was cured using ceramic binder, then reacted but not impregnated. The modulus of this composite is about 3.5 GPa. This will be the stiffness of the coil structure after reaction.

The Poisson's ratio measurements are shown in Fig. 5 in which the loading direction is azimuthal. Note that the compressive strain is taken as positive. The Poisson's ratio in azimuthal-axial direction ($\nu_{12}$=0.15) is smaller than in azimuthal-radial direction ($\nu_{32}$=0.45).

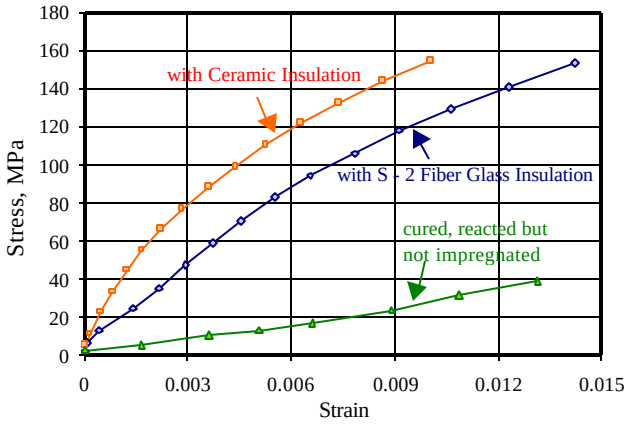


**Figure 4**: *Mechanical behavior of the composite in azimuthal direction at room temperature.*

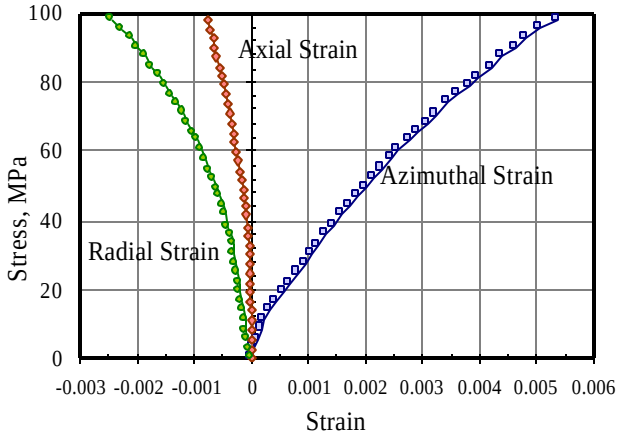


**Figure 5**: *Poisson's ratio measurements for the composite with ceramic insulation at room temperature.*

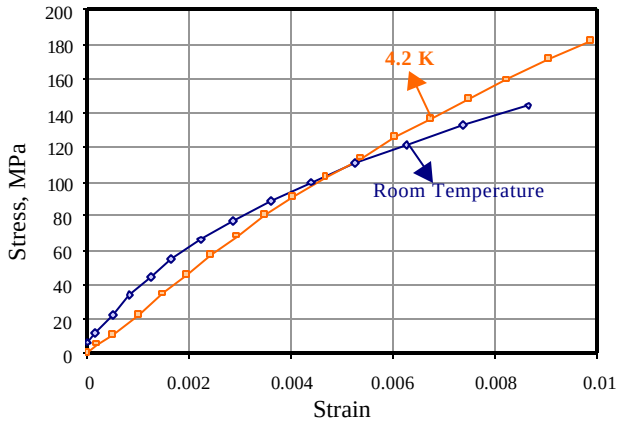


**Figure 6**: *Effect of temperature on the mechanical behavior of the composite with ceramic insulation.*

The modulus measurements at 4.2 K (Fig. 6) indicate the there is no apparent increase in stiffness with decrease in temperature; except that the behavior at 4.2 K is more linear than at room temperature.

*B. Axial and Radial Directions: Monotonic Loading*

The mechanical response of the composite in the axial direction at room temperature and at 4.2 K is shown in Fig. 7. The composite behavior is quite linear unlike in azimuthal direction. The behavior of the composite with both the S-2 fiber glass and ceramic insulations was similar as the conductor behavior dominates in axial direction.

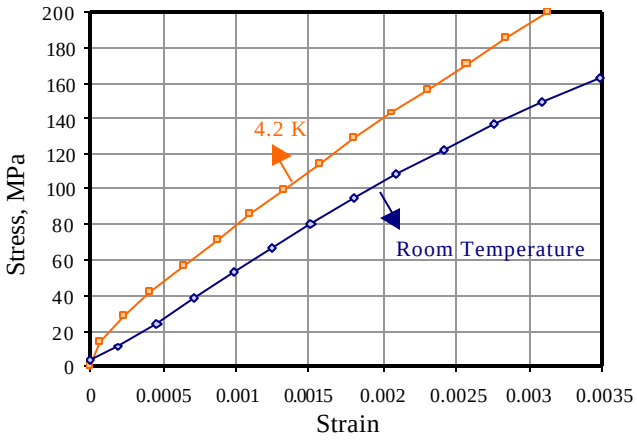


**Figure 7**: *Mechanical behavior of the composite in the axial direction.*

The mechanical response of the composite in the radial direction at room temperature is shown in Fig. 8. Note that the stiffness in the radial direction is much less than in axial direction. These experiments showed that the composite even after epoxy impregnation is very unstable in the radial direction especially when it is not confined in the azimuthal direction. Also shown in the figure is the behavior of the composite which was cured with the binder and then reacted but not impregnated.

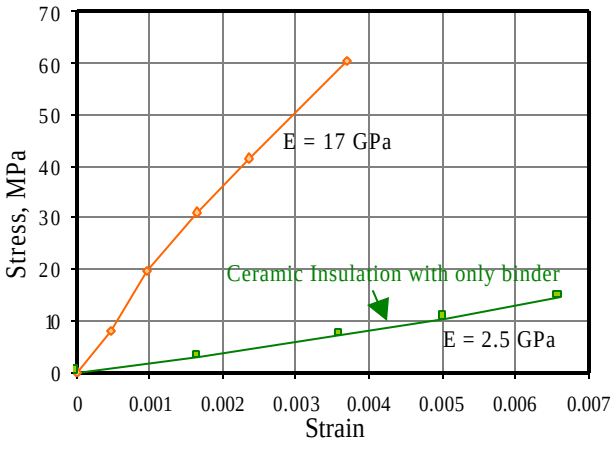


**Figure 8:** *Mechanical behavior of the composite at room temperature in radial direction.*

*C. Azimuthal Direction: Cyclic Loading*

As shown in the previous sections, the azimuthal mechanical behavior of the composite is non-linear; which makes the mechanics of the magnet much more complicated. In order to increase the stiffness of the composite which will also make the mechanical behavior more linear, cyclic loading tests were performed (Fig. 9). These results show that we could load the sample upto a peak stress and then unload which would then result in a composite with higher modulus and a linear mechanical behavior for subsequent loading cycles. However the initial loading leads to plastic deformation, the amount of which depends on the peak-stress. Note that the composite behavior will be linear in the re-loading cycles only upto the peak-stress in the initial cycle and once it is re-loaded beyond this stress the composite returns to its initial non-linear behavior with a lower modulus (see Fig. 10). Further the overall behavior of the composite under load-unload-reload tests is similar to that of the monotonic loading tests.

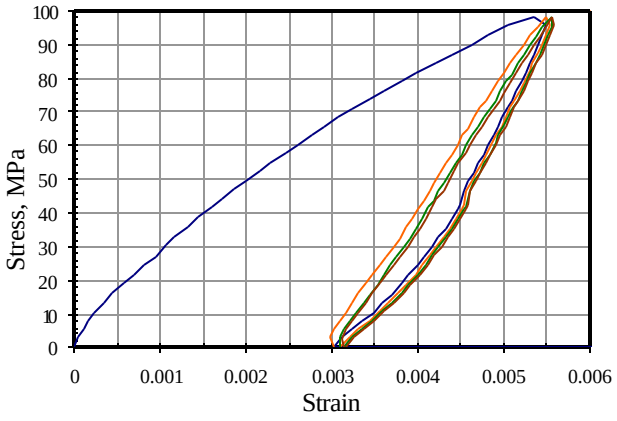


**Figure 9:** *Mechanical behavior of the composite in azimuthal direction under cyclic loading.*

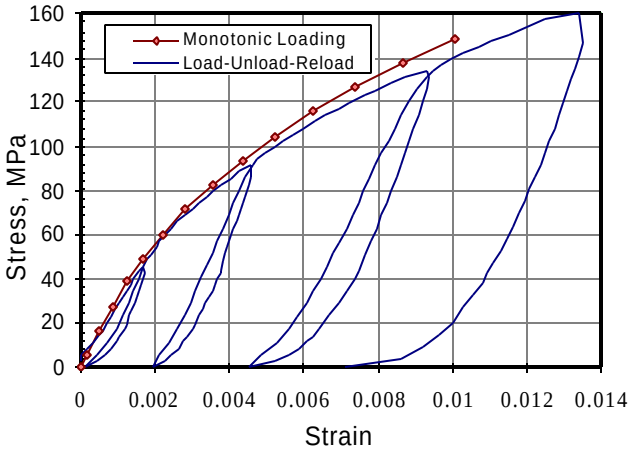


**Figure 10:** *Load-Unload-Reload tests on the composite at room temperature in azimuthal direction.*

The last series of tests were done in an attempt to simulate the loading sequence in an actual magnet. A ten-stack sample was tested in four cycles as shown in the Fig. 11. The first cycle simulates the "massaging" process at room temperature to increase the stiffness of the coil assembly. The second cycle also at room temperature corresponds to the loading of the coils during magnet assembly. The third cycle at 4.2 K represents the the changes in pre-stress with cool down and during excitation. The last cycle at room

temperature shows the warm-up behavior of the coil in the magnet. The composite behavior is quite linear after initial massaging with some hysteresis both at 300 K and at 4.2 K. Also the reloading moduli at both the temperatures are similar.

Finally cyclic loading had no effect on the stiffness in the axial direction as the composite exhibited linear behavior starting from the initial loading cycle without any residual plastic deformation.

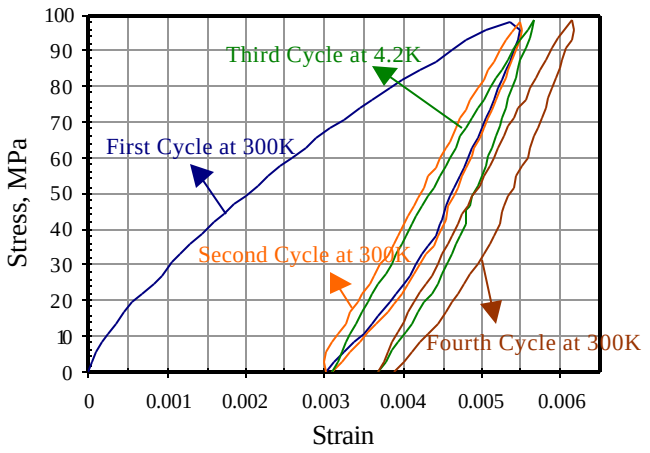


**Figure 11**: *Mechanical behavior of the composite with ceramic insulation for the loading sequence as seen in a magnet.*

## IV. THERMAL PROPERTIES

The integrated thermal contraction coefficient of the epoxy impregnated $Nb_3Sn$ composite in all the three directions was measured using a simple strain gage technique [6]. The temperature induced apparent strain in a sample, $\varepsilon_s$ due to change in temperature, $\Delta T$ is given by,

$$\varepsilon_s = \frac{\Delta R_s}{R F_G} = \left[\frac{\beta_G}{F_G} + (\alpha_s - \alpha_G)\right]\Delta T \qquad (1)$$

Where $\Delta R/R$ is the unit resistance change, $\beta_G$ is the thermal coefficient of resistance of grid material, $(\alpha_s - \alpha_G)$ is the difference in thermal coefficients between the sample and the grid respectively and $F_G$ is the gage factor. If the same type of gage is installed on a standard reference material with a known thermal coefficient, $\alpha_R$ then,

$$\varepsilon_R = \frac{\Delta R_R}{R F_G} = \left[\frac{\beta_G}{F_G} + (\alpha_R - \alpha_G)\right]\Delta T \qquad (2)$$

Subtracting the above two equations and rearranging we get,

$$(\alpha_s - \alpha_R) = \frac{(\varepsilon_s - \varepsilon_R)}{\Delta T} \qquad (3)$$

Knowing $\alpha_R$, $\varepsilon_s$ and $\varepsilon_R$ for a particular change in temperature, we can compute $\alpha_s$, the integrated thermal contraction coefficient of the sample. In the present study we used 304 stainless steel as a reference material and WK series of strain gages from MICRO MEASUREMENTS GROUP. Table 2 lists the integrated thermal contraction coefficients of the composite. To check the repeatability, four different composite samples were tested in axial direction upto 77 K and the values ranged between 2.26 to 2.32 µm/mm. Copper was also tested to compare with the already published data. Note that the published data for copper is 3.00 µm/mm from 300 K to 77 K [5].

| Material | $\alpha_1$ µm/mm | $\alpha_2$ µm/mm |
|---|---|---|
| 304 Stainless Steel [5] | 2.81 | 2.92 |
| Copper | 3.01 | 3.22 |
| Coil Azimuthal direction | 3.22 | 3.50 |
| Coil Axial and Radial directions | 2.29 | 2.59 |

**Table 2:** *Integrated thermal contraction measurements for copper and the impregnated composite. $a_1$ is from 300 to 77 K and $a_2$ is from 300 to 4.2 K.*

## V. SUMMARY

Ceramic insulation along with ceramic binder by CTD seems to be promising new development in cable insulation. The curing process can be used to define the shape and size of the coil before reaction. This process also simplifies the tooling requirements as it makes the coils easier to handle.

The thermo-mechanical properties of the impregnated composite have been investigated extensively. These properties are very essential to design and analyze the mechanical support structure for the magnet. Tables 3 and 4 summarize the mechanical properties under monotonic loading and after initial loading to 100 MPa.

| Material | $E_{Azimuthal}$, GPa | | $E_{Axial}$, GPa | |
|---|---|---|---|---|
| | 300 K | 4.2 K | 300 K | 4.2 K |
| $Nb_3Sn$ + Ceramic | 27 | 22 | 44 | 55 |
| $Nb_3Sn$ + S-2 Fiber | 18 | 26 | 47 | 56 |

**Table 3:** *Mechanical properties of the composite under monotonic loading conditions.*

| Material | E, GPa | | Poisson's Ratio |
|---|---|---|---|
| | 300 K | 4.2 K | |
| $Nb_3Sn$ + S-2 | 39 | 40 | $\nu_{12}$= 0.15; $\nu_{32}$= 0.34 |
| $Nb_3Sn$+ceramic | 38 | 38 | $\nu_{12}$= 0.14; $\nu_{32}$= 0.33 |

**Table 4**: *Azimuthal modulus and Poisson's ratio of the composite after massaging to 100 MPa.*

## REFERENCES


[1] G. Ambrosio, et al., "Development of the 11 T $Nb_3Sn$ Dipole Model at Fermilab", *MT-16*, Tallahassee, FL, 1999.

[2] J. Rice, et al., "Mechanical and Electrical Properties of Wrappable Ceramic Insulation", *IEEE Trans. on Applied Superconductivity*, Vol. 9, No. 2, pp. 220-223, June, 1999.

[3] D.R. Chichili, et al., "Investigation of Cable Insulation and Mechanical Properties of $Nb_3Sn$ composite", *Fermilab Preprint*, FERMILAB-Conf-99/052, April 1999.

[4] N. Andreev, et al., "Fabrication and Testing of High Field Dipole Mechanical Model", *MT-16*, Tallahassee, FL, 1999.

[5] Y. Iwasa, "Case Studies in Superconducting Magnets", Plenum Press, NY, 1994.

[6] "Strain Gage Technology: Thermal Expansion Measurement", Technical Note, TN-513, MICRO MEASUREMENTS GROUP.